Gyrokinetic modelling of light impurity peaking in JET baseline and hybrid H-modes: a missing ingredient?

P. Manas[1], Y. Camenen[1], S. Benkadda[1], H. Weisen[2], C. Angioni[3],
F. J. Casson[4], C. Giroud[4] , M. Gelfusa[5] and JET contributors*
EUROfusion Consortium, JET, Culham Science Centre, Abingdon, OX14 3DB, UK
[1] *Aix-Marseille Université, CNRS, PIIM UMR7345, 13397 Marseille, France*
[2] *CRPP, École polytechnique fédérale de Lausanne (EPFL), CH-1015 Lausanne*
[3] *Max-Planck-Institut für Plasmaphysik, D-85748 Garching, Germany*
[4] *CCFE, Culham Science Centre, Abingdon, OX14 3DB, UK*
[5] *Department of Industrial Engineering, University of Rome "Tor Vergata", via del Politecnico 1, Roma, Italy*

In this paper, quasilinear gyrokinetic modelling of the Carbon peaking factor in JET baseline and hybrid H-modes is presented. The study is based on a database of ~ 1800 shots (during the carbon wall era) covering a large range of plasma parameters: $I_p < 2.6MA, q(r) = 1.5-4, n_e = 2-6\cdot 10^{19}m^{-3}, P_{NBI} = 5-22MW, P_{ICRH} = 0-4MW$. High toroidal rotation cases with improved magnetic equilibrium reconstruction have been extracted (~ 156 shots) leading to a reduced database previously used for momentum transport studies [1]. The objective of the present work, based on the reduced set, is twofold: can the modelling approach be validated against experimental data and is toroidal rotation an important ingredient for light impurity transport as shown on ASDEX Upgrade [2].

Before addressing these questions, the robustness of the carbon density profiles, provided by the Charge Exchange Recombination Spectroscopy (CXRS) diagnostic [3] (using the C5+ N=8 to 7 line), and of their radial gradients is assessed by performing multiple fits using gaussian noise with experimental error bars as standard deviation. A small deviation for the radial coordinate has also been used. In Fig. 1, the corresponding fitted profiles of carbon density and logarithmic density gradient (R/L_{n_c}) are shown using or not the outer localised radial experimental value. The choice of including or not this last experimental point is motivated by the larger uncertainties on the neutral beam attenuation (linked to the pedestal width and position) and hence on the deduced carbon density. Furthermore, it has been observed that taking into account this last point leads to a strong correlation between R/L_{n_c} and the shot number over physically relevant parameters for cases close to the edge ($\rho \geq 0.8$). In the following, a detailed comparison between modelled and experimental carbon peaking factor is presented at $\rho = 0.65$ where R/L_{n_c} is negative (outward pinch velocity) and the fitted gradients are robust with respect to fitting

hypotheses.

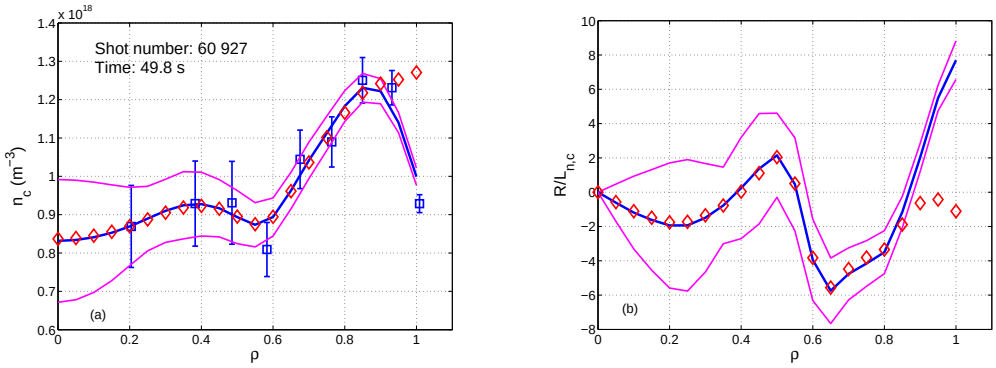

Figure 1: Carbon density (a) and logarithmic density gradient (b) profiles. Fitted profiles using the outer localised radial experimental point (blue line) or not (red diamonds) are shown together with error bars for the former (pink lines). Experimental data are represented by blue squares.

The modelling of the carbon peaking factor is performed using the flux-tube version of the gyrokinetic code GKW [4] which includes centrifugal effects and realistic magnetic equilibrium to compute the turbulent impurity flux. Neoclassical contributions to this peaking factor are evaluated using the neoclassical code NEO and found to be negligible compared to turbulent transport (a factor of ~ 100 between the neoclassical and turbulent diffusivities). A quasilinear approach is chosen to tackle the large number of experimental data. Using a mixing length rule [5], the quasilinear particle flux can be written as follows:

$$\Gamma_{QL} = \sum_{k_\theta} \Gamma_{k_\theta} \frac{\gamma_{k\theta}}{< k_\perp^2 >} \qquad \text{with} \qquad < k_\perp^2 >= \frac{\int |\phi|^2 k_\perp^2 \, \mathrm{d}s}{\int |\phi|^2 \mathrm{d}s} \tag{1}$$

with $\gamma_{k\theta}$ the growth rate of the linear instability at the poloidal wave number k_θ, ϕ the electrostatic potential, s the field aligned coordinate and $k_\perp$ the local perpendicular wave vector. The normalised impurity flux is decomposed in a diffusive and a convective part:

$$\frac{R\Gamma_{QL}}{n} = D_{QL}\frac{R}{L_n} + RV_{QL} = D_{QL}\left(\frac{R}{L_n} + C_{T,QL}\frac{R}{L_T} + C_{u,QL}u' + C_{p,QL}\right) \tag{2}$$

with R the major radius, u' the normalised gradient of toroidal rotation frequency ($R^2\nabla\Omega/v_{th,i}$), D a diffusion coefficient and V the pinch velocity consisting of three terms: thermo-diffusion ($C_T\frac{R}{L_T}$), roto-diffusion ($C_u u'$) and a constant (C_p). Since there is no source of carbon in the core, the steady state carbon particle flux is zero, hence giving a direct relation for the quasilinear logarithmic density gradient $R/L_{n_c} = -RV_{QL}/D_{QL}$.

In Fig. 2 experimental and modelled carbon peaking factor are represented against the normalised gradient of toroidal rotation frequency u' and the normalised collisionality ν_* for cases without ICRH at $\rho = 0.65$ (ICRH can induce significant carbon poloidal asymmetries and these cases are left for another study). The predicted R/L_{n_c} is also shown neglecting roto-diffusion,

underlining the importance of this term in recovering negative experimental carbon peaking factor at high u'. In Fig. 2b, a marked dependency of experimental $R/L_{n,c}$ against the neoclassical collisionality ν_* is observed which does not appear for the modelled $R/L_{n,c}$. Furthermore, while modelled and experimental carbon peaking factor are in agreement within experimental error bars at low ν_* (< 0.03), a clear difference is seen at higher ν_*. Variations of physical parameters used in gyrokinetic simulations such as the safety factor ($\pm 50-100\%$), the magnetic shear ($\pm 50\%$), the toroidal velocity ($\pm 50-100\%$) and its gradient ($\pm 50-100\%$), the logarithmic temperature ($\pm 15\%$) and density gradients ($\pm 20\%$) do not make it possible to recover such high negative values of the carbon peaking factor. Several mixing length rules have also been tested together with finite radial wave numbers k_x, changing the spectral shape to increase higher or lower $k_\theta \rho_i$ contributions.

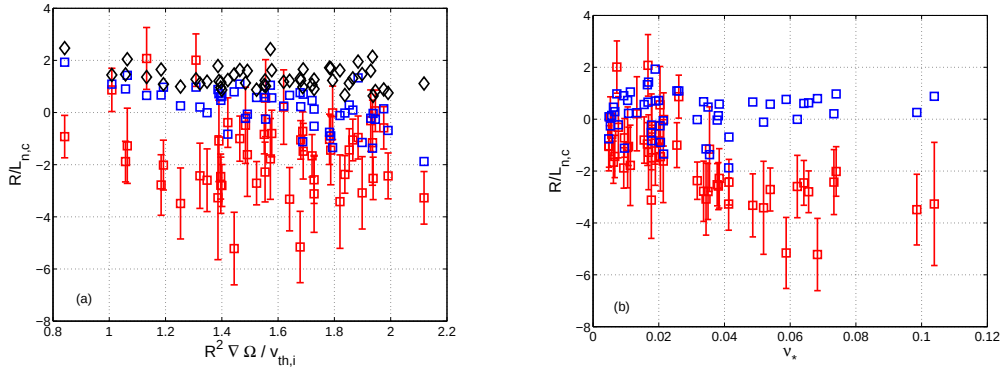

Figure 2: Modelled carbon peaking factor (blue squares) and experimental values (red squares) versus the normalised gradient of toroidal rotation frequency (a) and ν_* (b). Cases without roto-diffusion are also represented (black diamonds).

To better characterise this ν_* dependency, multilinear regressions are performed on experimental and modelled R/L_{n_c} (Fig. 3) with the following physically relevant set of parameters: R/L_n, R/L_{T_i}, R/L_{T_e}, T_i/T_e, u', $R\Omega/v_{th,i}$, q, $\hat{s}$, Z_{eff}, ν_*, β. The regressed R/L_{n_c} is computed using 3 variables with their coefficients b, uncertainty δb and the statistical significance (STS) $b/\delta b$ (see [1] for more details). The expression for the regressed R/L_{n_c} is then of the form:

$$\frac{R}{L_{n_c}} regressed = b_1 var_1 + b_2 var_2 + b_3 var_3 + constant \tag{3}$$

Using this decomposition, a set of fits are obtained with increasing standard deviation σ. In Fig. 3 regressions for only one set of 3 variables is represented. For the 5 best fits (minimum standard deviation) recurring parameters for both modelled and experimental R/L_{n_c}, u' and R/L_n are always obtained (Fig. 3a, 3c) while the third variable can be either T_i/T_e, R/L_{T_i}, $R\Omega/v_{th,i}$ or the magnetic shear. This dependence in u' and R/L_n is very similar in magnitude (linear coefficients b) with a lower value for modelled R/L_{n_c}. In Fig. 3b and 3d, R/L_n has been suppressed from the set of parameters unraveling the strong dependency of the experimental

carbon peaking factor and ν_* (ν_* and R/L_n are strongly correlated). This dependence in ν_* is less pronounced for modelled R/L_{n_c} which is consistent with results of Fig. 2. It is also interesting to note that the coefficients in front of R/L_{T_i} (linked to thermo-diffusion) are similar for experimental and modelled carbon peaking factor.

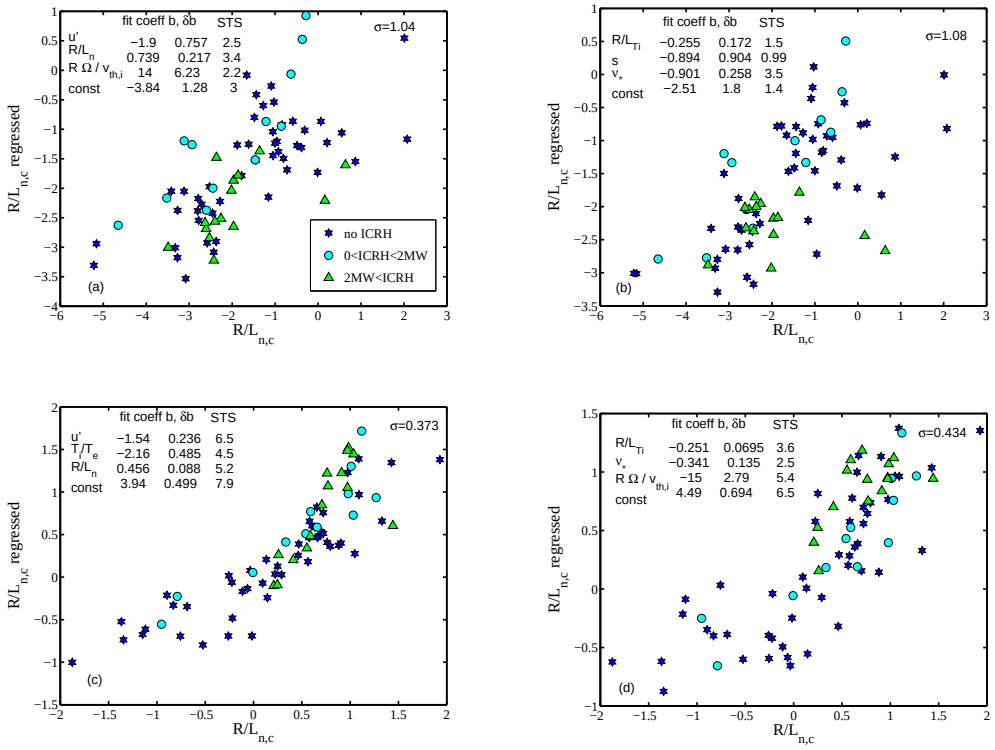

Figure 3: Multilinear regression of the experimental (a,b) and modelled (c,d) carbon peaking factor at $\rho = 0.65$.

To conclude, provided roto-diffusion is included, a rather good prediction of the carbon peaking factor at high gradient of toroidal rotation frequency and low ν_* is observed for this JET H-modes database, using quasilinear gyrokinetic simulations (neoclassical contributions are negligible). However the calculations fail to predict high negative experimental R/L_{n_c} at high ν_*. Multilinear regressions of modelled and experimental R/L_{n_c} help identifying the relevant parameters and confirm a stronger dependence on ν_* for experimental R/L_{n_c} than in the modelling. This work has been carried out within the framework of the EUROfusion Consortium and has received funding from the Euratom research and training programme 2014-2018 under grant agreement No 633053. The views and opinions expressed herein do not necessarily reflect those of the European Commission.

References

[1] H. Weisen *et al*, Nuclear Fusion **52**, 042001 (2012)
[2] F. J. Casson *et al*, Nuclear Fusion **53**, 063026 (2013)
[3] C. Giroud *et al*, Review of Scientific Instruments **79**, 10F525 (2008)
[4] A. G. Peeters *et al*, Computer Physics Communications **180**, 2650 (2009)
[5] F. Jenko, T. Dannert and C. Angioni, Plasma Phys. Control. Fusion **47**, B195 (2005)

*See the Appendix of F. Romanelli et al., Proceedings of the 25th IAEA Fusion Energy Conference 2014, Saint Petersburg, Russia